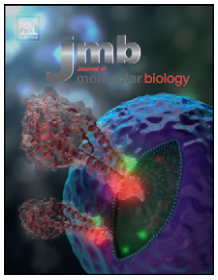
Communication



# The Cytoplasmic Domain of the T-Cell Receptor zeta Subunit Does Not Form Disordered Dimers

**Amanda Nourse and Tanja Mittag**

***Structural Biology,*** *St. Jude Children's Research Hospital, 262 Danny Thomas Place, MS 311, Memphis, TN 38105, USA*

***Correspondence to Tanja Mittag:*** *tanja.mittag@stjude.org*
http://dx.doi.org/10.1016/j.jmb.2013.09.036
***Edited by P. Wright***

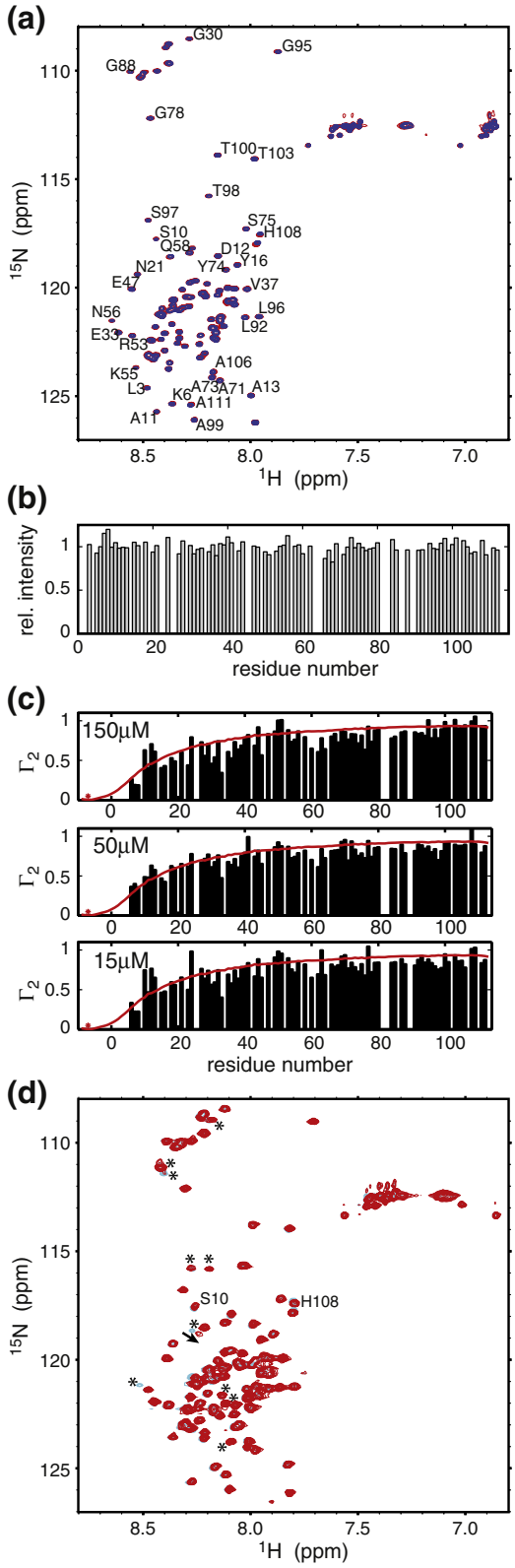
## Abstract

Intrinsically disordered regions in proteins play active roles in recognition, signaling and molecular sorting. They often undergo coupled folding and binding giving rise to largely ordered interfaces with their binding partners. The cytoplasmic region of the T-cell receptor zeta subunit ($\zeta_{cyt}$) has been previously proposed to specifically dimerize in the absence of a disorder-to-order transition, suggesting an intriguing dimerization mechanism that may involve multiple transient interfaces. We show here using analytical ultracentrifugation, NMR, size-exclusion chromatography (SEC) and multi-angle light scattering that neither $\zeta_{cyt}$ nor the cytoplasmic region of CD3ε significantly populates a dimeric state but that they are mostly monomers in solution up to millimolar concentrations. They experience a salt- and concentration-dependent shift of their elution volume in SEC previously interpreted as dimerization. Our data show that $\zeta_{cyt}$ does not form a highly disordered protein complex and leaves open the question as to whether completely disordered dimers (or other oligomers) exist in nature.
© 2013 Elsevier Ltd. All rights reserved.

## Introduction

Intrinsically disordered proteins (IDPs) and IDP regions are common in eukaryotic proteins [1,2] and are often more than simple linkers between domains. They play active roles in recognition, signaling and molecular sorting [3–5]. IDP regions are generally accepted to interact with their binding partners through coupled folding and binding [6,7]. Their relative lack of hydrophobic residues and intramolecularly stabilizing interactions prevents them from folding on their own [8], but they fold efficiently on complementary surfaces of specific binding partners [9]. Recent work has demonstrated that some IDPs retain functional disorder even in complexes [10]. What is the functional advantage of these so-called "fuzzy" complexes? (The term "fuzzy" complex derives from "fuzzy" logic and is supposed to indicate the possibility of signaling outputs between 0 and 1 made possible by the conformational complexity in the complex. As this concept does not necessarily apply to all such complexes, we use "fuzziness" to describe conformational disorder in the bound state.) In the most striking examples, disorder is not restricted to regions flanking binding motifs but extends into the binding interface through fraying of the ends of bipartite motifs [11], dynamic interactions of several motifs in an IDP with a given binding partner [12–14] or self-organization of elastomeric proteins into highly hydrated, largely disordered aggregates [15]. Well-described examples are the dynamic interactions of the regulatory region of the cystic fibrosis transmembrane regulator with other domains of the protein [12] and of the yeast cyclin-dependent kinase inhibitor Sic1 with the substrate recognition subunit of its ubiquitin ligase, Cdc4 [13,16]. Sic1 harbors nine phosphorylation-dependent binding motifs for Cdc4, each of which interacts with a single binding pocket in Cdc4, one at a time, in a dynamic equilibrium [13]. Although each motif is ordered when engaged, each motif is disordered in the complex a significant part of the time while other motifs are engaged. The resulting disorder and conformational averaging in the complex presumably allows Cdc4 to sense the phosphorylation state of Sic1 through polyelectrostatic interactions [17] and read out the cell cycle status of the cell in an ultrasensitive manner [18,19]. In contrast, a single binding motif and a stable interaction generated through coupled folding and binding would be

expected to produce a graded response. In the case of the Sic1/Cdc4 complex, the function of disorder in the complex is well understood but, in other cases, may be less obvious and difficult to demonstrate directly.




An interesting related but more general question is: how disordered a biologically functional fuzzy complex can be. An often cited example [4,10,20–26] for a highly fuzzy complex is the putative dimer formed by the cytoplasmic domain of the T-cell receptor zeta subunit ($\zeta_{cyt}$) [27]. Indeed, Sigalov *et al.* reported that the intracellular domains of several immune receptor subunits, including Igα, Igβ, IGE, CD3γ, CD3δ, CD3ε and T-cell receptor zeta, dimerize in solution *in vitro* [27]. Of these immune receptor domains, $\zeta_{cyt}$ was investigated in most detail and was reported to have a monomer–dimer dissociation constant of ~10 μM and a dimer–tetramer dissociation constant of ~1 mM. Affinities at least in the micromolar range may have biological relevance because clustering of T-cell receptor subunits through extracellular ligands [28] and pre-clustering even in their absence are suggested to lead to high local concentrations of intracellular domains [29].

NMR spectra of $\zeta_{cyt}$ at low and high micromolar concentrations, at which $\zeta_{cyt}$ is expected to exist mostly as either monomer or dimer, respectively, were

**Fig. 1.** $\zeta_{cyt}$ $^{1}H,^{15}N$ HSQC spectra under different conditions reported on a monomeric state. (a) $^{1}H,^{15}N$ HSQC spectra of 10 μM (blue) and 400 μM (red) $\zeta_{cyt}$ are highly similar. (b) The comparison of scaled resonance intensities at 10 and 400 μM $\zeta_{cyt}$ as a function of residue number shows no sequence-specific broadening. (c) PRE profiles of spin-labeled $\zeta_{cyt}$ show transient intramolecular rather than intermolecular contacts. Γ2 for $\zeta_{cyt}$ MTSL spin-labeled at position −7 (marked by an asterisk) as a function of protein concentration (150 μM, top; 50 μM, middle; 15 μM, bottom) was calculated from intensity ratios of a paramagnetic and diamagnetic sample pair [43], the latter obtained by reduction with 10-fold excess of ascorbic acid. The red continuous lines represent the expected PRE profiles for a random coil model of the protein calculated from a 100,000 conformer ensemble generated with flexible-meccano [44]. (d) Disulfide-linked $\zeta_{cyt}$ shows no evidence of a dimerization interface because HSQC spectra of reduced (cyan) and disulfide-linked $\zeta_{cyt}$ (red) are identical except for linker region signals. Resonances unique to Cys-$\zeta_{cyt}$ and absent from wild-type $\zeta_{cyt}$ are marked by asterisks; one linker serine resonance with chemical shift perturbation upon Cys cross-linking is marked with an arrow. Disulfide-linked $\zeta_{cyt}$ was obtained by oxidation with tetrathionate [45] and subsequent preparative SEC. NMR assignments are taken from Jaravine *et al.* [31]. $\zeta_{cyt}$ was in 20 mM potassium phosphate (pH 6.2), 1 mM ethylenediaminetetraacetic acid (EDTA), 0.5 mM benzamidine and 90% $H_2O$/10% $D_2O$. Gradient-selected, sensitivity-enhanced HSQC spectra were recorded at 288 K on a Bruker Avance 600-MHz NMR spectrometer with a TCI triple-resonance cryogenic probe with 1024 × 128 complex data points and varying number of scans to account for the different protein concentrations and sensitivity. Data processing was performed in TopSpin (Bruker BioSpin), and spectral analysis was performed in Sparky (Goddard, T.D. and Kneller, D.G., University of California, San Francisco).

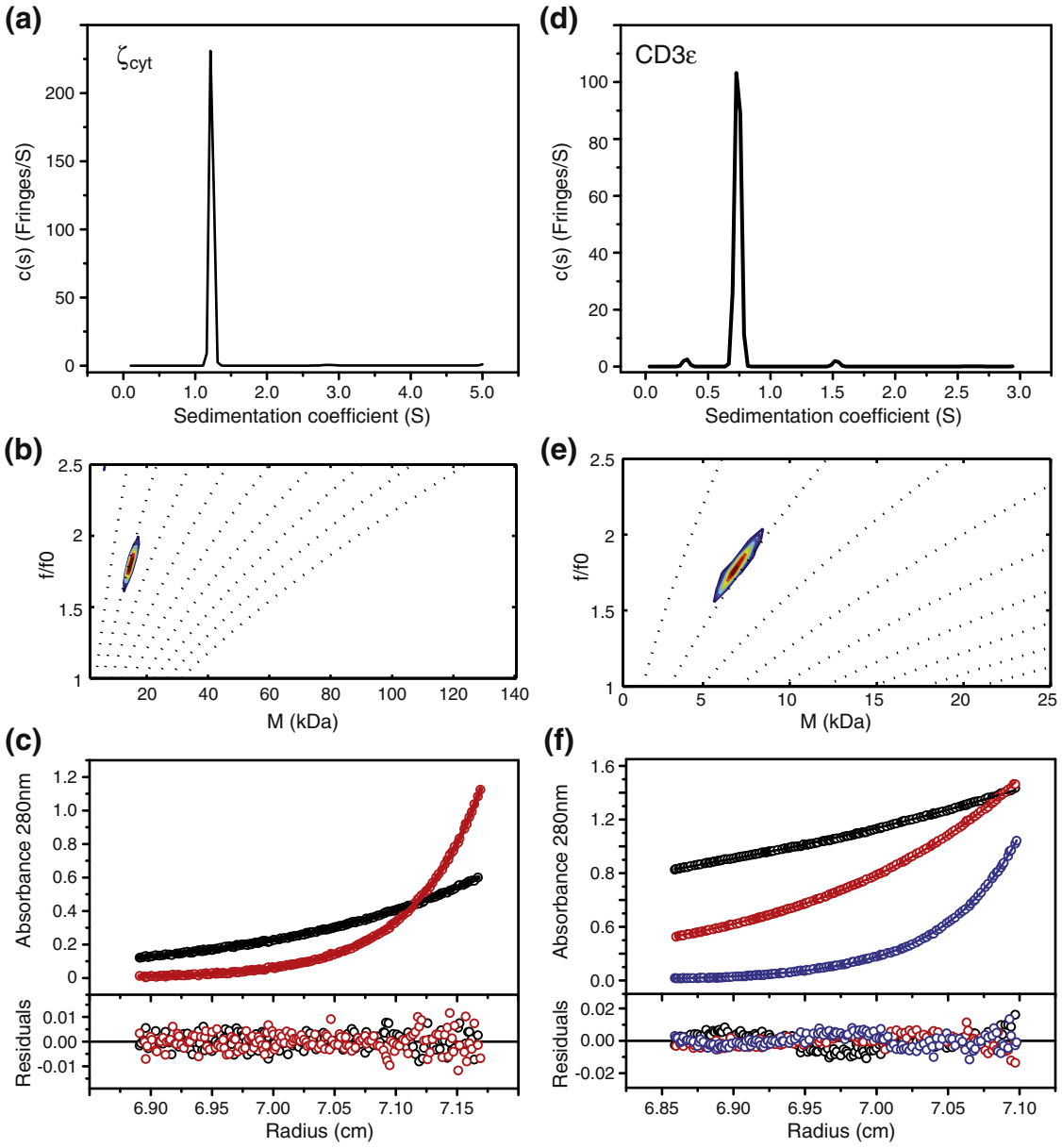



**Fig. 2.** $\zeta_{cyt}$ and CD3ε are mostly monomeric. SV (a, b, d and e) and SE (c and f) experiments were carried out in PBS (*p*hosphate-*b*uffered *s*aline; pH 7.0), 1 mM EDTA and 1 mM benzamidine for $\zeta_{cyt}$ (left) and in PBS (pH 7.0) for CD3ε (right). (a and d) Continuous sedimentation coefficient distribution model $c(s)$ and (b and e) two-dimensional size-and-shape distribution analyses of SV data of (a and b) 340 μM $\zeta_{cyt}$ and (d and e) 290 μM CD3ε. Shown are contour plots of $c(M,f/f_0)$ of the transformed velocity data with 0 fringes/S (white) to maximum value fringes/S (red), with increasing color temperature indicating higher values. Velocity data were acquired at 20 °C at a rotor speed of 50,000 rpm and indicate only one species in solution close to the monomer M [34,35]. (c and f) Fringe displacement profiles at equilibrium for 140 μM, 80 μM and 20 μM and absorbance scans at 280 nm for (c) 20 μM $\zeta_{cyt}$ were analyzed globally (for the profiles at all concentrations, see Fig. S2), and absorbance scans at 280 nm for (f) 290 μM CD3ε are plotted *versus* the distance from the axis of rotation (radius). $\zeta_{cyt}$ was centrifuged at 20 °C at increasing speeds of 22,000 rpm (black, 32 h) and 38,000 rpm (red, 23 h); CD3ε was centrifuged at 4 °C at increasing speeds of 18,800 rpm (black, 46 h), 31,800 rpm (red, 38 h) and 54,000 rpm (blue, 22 h). The continuous lines represent the global nonlinear least squares best fit of all the data sets to a reversible monomer–dimer self-association model yielding $K_D$ values of 6.2 and 8.3 mM, respectively (see Supplemental Methods for more detailed information).

**Table 1.** SE analysis of $\zeta_{cyt}$ and CD3ε according to a single-species model, a two-discrete-species model or a monomer–dimer self-association model

| Sample | Concentration (μM)[a] | M[b] (kDa) | rmsd[c] | M[d] (kDa) | rmsd[c] | $K_D$ (mM)[e] | rmsd[c] |
|---|---|---|---|---|---|---|---|
| $\zeta_{cyt}$ | 20, 80, 140 | 14.712 | 0.0065 | 28.013 | 0.0051 | 6.2 | 0.0061 |
| CD3ε | 290 | 6.689 | 0.0037 | 17.090 | 0.0033 | 8.3 | 0.0043 |

[a] Total protein loading concentrations are in micromolar units; proteins are in PBS (pH 7), 1 mM EDTA and 1 mM benzamidine.
[b] Single-species model with mass the average M.
[c] rmsd with units in interference or absorbance and, for the global analysis, the average rmsd of all the data sets.
[d] Molecular mass of the second species in a two-discrete-species model: first species is fixed to 13.157 kDa, and the fraction of the second species is ~0.5%.
[e] Dissociation equilibrium constant $K_D$ for the reversible monomer–dimer self-association model; M is fixed to the theoretical value.

reported to be identical [30]. This result was taken as evidence that the dimer remains fully disordered [30]. A stable dimer interface would result in differences in chemical shift and line width between monomeric and dimeric $\zeta_{cyt}$. Speculation into the mechanism of dimerization led to a model in which several different interfaces are sampled in a dynamic equilibrium, giving rise only to small chemical shift or intensity differences that may only be observed in NMR spectra upon close inspection [23]. We used complimentary biophysical techniques to test the hypothesis that $\zeta_{cyt}$ forms disordered dimers through multiple interfaces.

## $\zeta_{cyt}$ is a monomer in solution

We first acquired $^{1}H,^{15}N$ heteronuclear single quantum coherence (HSQC) spectra of $\zeta_{cyt}$ at 10 and 400 μM concentrations (Fig. 1a). Indeed, the spectra are nearly identical with each other and to the spectra reported by Sigalov *et al.* [30]. Comparison of resonance intensities under the two conditions did not reveal localized broadening or candidate dimerization interfaces (Fig. 1b; assignments reported by Jaravine *et al.* [31]). To increase the sensitivity of NMR experiments toward the detection of transient interactions [32], we spin-labeled $\zeta_{cyt}$ with *S*-(2,2,5,5-tetramethyl-2,5-dihydro-1*H*-pyrrol-3-yl) methyl methanesulfonothioate (MTSL) on a cysteine residue introduced to the N-terminus and measured the paramagnetic relaxation enhancement (PRE) of amide protons along the sequence (Fig. 1c and Fig. S1). The PRE profile shows a strong PRE effect close to the labeling position where signals are broadened beyond detection, and the effect decreases gradually with increasing distance in primary sequence from the labeling position. The profile is close to that expected for a random coil chain (red lines) with additional weak PRE effects observed around position 60. To distinguish between intramolecular and intermolecular interactions as a source of these additional PRE effects, we measured PRE effects as a function of protein concentration. The close similarity of the profiles at different concentrations demonstrates that the PRE effects of residues far away from the labeling position in primary sequence are caused by intramolecular rather than by intermolecular interactions. Thus, $\zeta_{cyt}$ exhibits transient structure, but we did not observe signs of even transient dimerization.

To test the possibility of a much weaker self-association than previously reported, we increased the local concentration of $\zeta_{cyt}$ by disulfide cross-linking the N-termini, which usually connect to the transmembrane domain. We chose this orientation to mimic the condition of clustered T-cell receptor at the membrane, where a $\zeta_{cyt}$ dimer may have biological relevance. We cross-linked two molecules through an N-terminal cysteine attached via a glycine/serine-rich linker (denoted Cys-$\zeta_{cyt}$). The NMR spectra of Cys-$\zeta_{cyt}$ and disulfide-linked Cys-$\zeta_{cyt}$ differ only in the glycine and serine resonances adjacent to the cysteine/cystine (Fig. 1d). These data demonstrate that $\zeta_{cyt}$ does not self-associate when spatial constraints at the membrane are mimicked, via neither an ordered nor a disordered dimer.

Next, we investigated the oligomerization state of $\zeta_{cyt}$ by sedimentation velocity (SV) analytical ultracentrifugation (AUC), a technique that does not require calibration relative to proteins of known molecular mass (M) [33,34]. SV demonstrated that most of the protein existed as a monomer (Fig. 2a and b) as evident from a single peak in a continuous sedimentation coefficient distribution model *c*(*s*) (Fig. 2a) and in a two-dimensional size-and-shape distribution analysis [35] (Fig. 2b). The experimental M was slightly larger than the theoretical (M =13,157 Da and confirmed by electrospray ionization mass spectrometry; see Fig. S2). This indicated the possibility of weak self-association, which we probed via sedimentation equilibrium (SE) AUC. SE is independent of protein shape and is the classical method to rigorously characterize biomolecular oligomerization [33,34]. The centrifugal forces generate a concentration gradient of the loading material in the cell and therefore probe oligomerization in a concentration range much broader than the loading concentrations. Even weak oligomerization can thus be observed with ease. In contrast to Sigalov *et al.* [27], we observed sedimentation behavior indicative of mostly monomers (Fig. 2c). A single-species model fit well but resulted in an M that was slightly larger than

the theoretical (Table 1). The data did not fit to a monomer-dimer-tetramer self-association model, excluding the possibility of tetramerization. A global fit of SE data from three different protein concentrations to a reversible monomer–dimer self-association model resulted in a dissociation constant of 6.2 mM (Fig. 2c, Table 1 and Fig. S3), that is, nearly 3 orders of magnitude weaker than that reported by Sigalov *et al.*

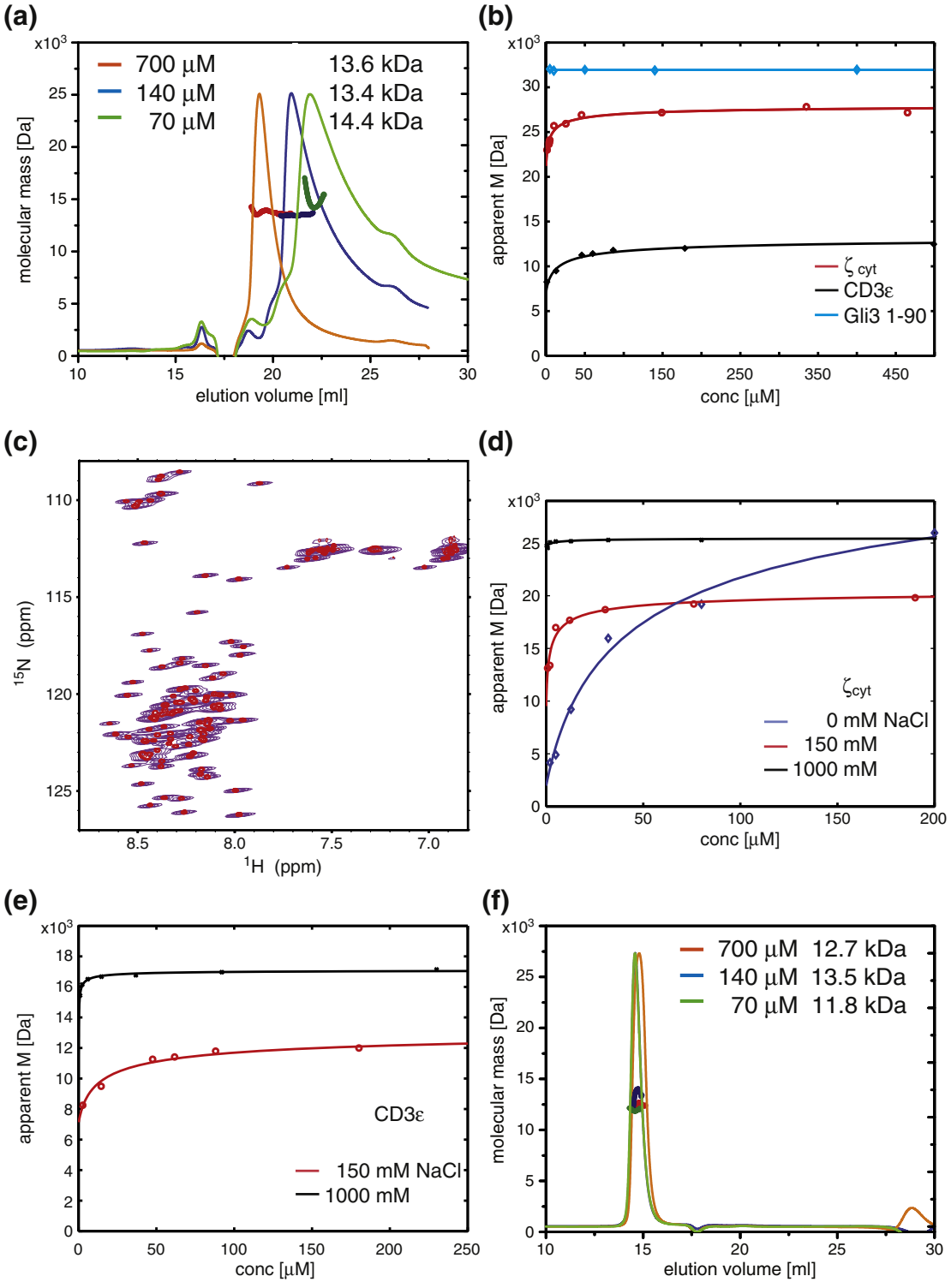



**Fig. 3** *(legend on next page)*

[27]. At a micromolar $\zeta_{cyt}$ concentration, for example, 10 μM, only a fraction of 0.35% of $\zeta_{cyt}$ would be dimeric at a $K_D$ of 6 mM (compared to a fraction of 50% with a $K_D$ of 10 μM; see Fig. S4). The data can alternatively be fit equally well to a two-discrete-species model in which the first species' M was fixed to 13,157 Da and the second was floated and fit to ~28,000 Da at a fraction of ~0.5% (Table 1). Although even weak self-association may be biologically relevant in clustered TCRs, the lack of interactions between protomers in disulfide-linked Cys-$\zeta_{cyt}$ demonstrates that $\zeta_{cyt}$ does not dimerize even at extremely high local concentrations and that the AUC data likely report on a low concentration contaminant. We consistently observed nearly exclusively $\zeta_{cyt}$ monomers up to millimolar concentrations with AUC at 277 and 298 K and in 10 mM phosphate buffer with 10 mM or 150 mM added NaCl.

As dimerization had been reported also for other immune receptor cytoplasmic domains [27], we next probed the oligomeric state of CD3ε with AUC. We again observed monomers in SV and SE experiments even at high concentrations and a dissociation constant of 8.3 mM when we forced a fit to a reversible monomer–dimer self-association model (Fig. 2d–f and Table 1), suggesting that there was at most very weak, if any, dimerization. Hence, NMR and AUC data demonstrated that both $\zeta_{cyt}$ and CD3ε are mostly monomers in solution even up to millimolar concentrations.

## $\zeta_{cyt}$ exhibits a concentration-dependent shift of its elution volume in SEC

Next, we investigated the hydrodynamic properties of $\zeta_{cyt}$ as a function of concentration by size-exclusion chromatography (SEC) and the absolute M of the eluting species by coupled multi-angle light scattering (MALS) [36]. $\zeta_{cyt}$ consistently elutes as a monomeric species. Surprisingly, the elution volume ($V_{el}$) changes as a function of concentration (Fig. 3a). Importantly, the polydispersity was between 1.000 and 1.002, confirming that $\zeta_{cyt}$ elutes as a homogenous species and not a mixture of different oligomeric states. As MALS measures the weight-average M, even a small amount of dimer, oligomer or aggregate would increase the measured M significantly. At the lowest protein concentration (70 μM), the M is higher in the slopes of the peak in the MALS profile (Fig. 3a). This is often indicative of a small amount of sticky aggregate that elutes in a long tail extending into later peaks in the chromatogram. At higher concentrations, $\zeta_{cyt}$ elutes in a single, narrow peak. These data demonstrate unequivocally that $\zeta_{cyt}$ is a monomer in the concentration range covered (70–700 μM) but that it may surprisingly be prone to aggregation at low protein concentration. The shift of $V_{el}$ as a function of protein concentration was puzzling, and as it may have been previously interpreted as a sign of self-association, we investigated it further.

Sigalov *et al.* reported that $\zeta_{cyt}$, at a high loading concentration of above 400 μM, elutes at a retention time typical for an ~27-kDa folded protein, that is, at approximately the M of a $\zeta_{cyt}$ dimer [27]. Lowering the loading concentration progressively shifted the elution volume to larger values until reaching the M of the monomer. Although IDPs usually have larger hydrodynamic radii than folded proteins, the authors used folded proteins as standards to calibrate the MM to the retention volume of the column. We took a similar approach and also observed a shift of the elution volume to higher values, that is,

**Fig. 3.** The SEC concentration dependency of $\zeta_{cyt}$ and CD3ε is not caused by dimerization. (a) SEC-MALS profiles demonstrate the monomeric state of $\zeta_{cyt}$ despite the concentration dependency of $V_{el}$. We injected 100 μl of $\zeta_{cyt}$ at 700 μM (red), 140 μM (blue) and 70 μM (green) concentration with an autosampler onto a Shodex KW-803 gel-filtration column (with guard column) equilibrated in 20 mM potassium phosphate buffer (pH 7) and 1 mM EDTA, with 150 mM NaCl and the protein in the eluent detected by UV and a Wyatt DAWN-HELEOS MALS detector with a laser at 658 nm wavelength. SEC-MALS data plotted as a molecular mass distribution superimposed on the chromatogram of absorbance at 280 nm as a function of elution volume. (b) We injected 100 μl sample of $\zeta_{cyt}$, CD3ε or Gli3 1–90 at a given concentration from a dilution series onto a Superdex 75 10/300 gel-filtration column in PBS (pH 7) and 1 mM EDTA at 0.7 ml/min; its elution volume ($V_{el}$) was monitored and converted into an apparent molecular mass ($M^{app}$) based on calibration with globular protein standards (BioRad Gel-Filtration Standard) under given buffer conditions. The continuous lines serve to guide the eye. The injection loops were overfilled with 1.5× their volume to prevent a change in $V_{el}$ due to inconsistent injection. (c) $^{1}H$, $^{15}N$ HSQC spectra of 400 μM (red) $\zeta_{cyt}$ in buffer and (purple) in P-6DG gel-filtration resin have nearly identical chemical shifts. Resonances of $\zeta_{cyt}$ in resin are broad due to motional restriction under spatial confinement. $\zeta_{cyt}$ was in 20 mM potassium phosphate (pH 6.2), 1 mM EDTA, 0.5 mM benzamidine and 90% $H_2O$/10% $D_2O$. In case of P6-DG, 50 mM NaCl was added to prevent non-specific interactions with the resin. The amount of resin required to pack a 500 μl, gel-filtration column was hydrated in an excess of $\zeta_{cyt}$ solution for several hours and then transferred to a 5-mm NMR tube that was centrifuged to pack the resin and to remove trapped air bubbles. The supernatant was removed. (d and e) The proteins' apparent Ms were investigated under different salt concentrations. We injected 50 μl of (c) $\zeta_{cyt}$ or (d) CD3ε onto a Shodex KW-803 gel-filtration column; the $M^{app}$ was calculated based on careful calibration under given buffer conditions. Buffers were 20 mM potassium phosphate (pH 7) and 1 mM EDTA with NaCl varying between 0 and 1000 mM as indicated. (f) SEC-MALS profiles as in (a) with 1 M NaCl in the buffer.

smaller apparent molecular mass ($M^{app}$) upon lowering the loading concentration on a Superdex 75 10/300 gel-filtration column (GE Healthcare) (Fig. 3b). The shift was not as large as that reported by Sigalov *et al.*, but the data could be fit to a monomer–dimer equilibrium with a dissociation constant of 1 μM. The $M^{app}$ of the monomer and the dimer obtained by the fit were 21,000 and 28,000 Da, respectively, requiring a considerable compaction upon dimerization if the shift was indeed caused by self-association. CD3ε showed a similar concentration dependence of its elution volume and its $M^{app}$ (Fig. 3b).

We considered the following causes for the apparent disagreement between SEC and other biophysical data: (1) confinement-induced dimerization of $\zeta_{cyt}$ and CD3ε in the gel-filtration matrix but not free in solution, (2) overloading of the gel-filtration column accompanied by exclusion of protein molecules from appropriate pore sizes and premature elution, (3) interaction with the gel-filtration resin or other parts of the column and (4) non-ideal protein behavior that leads to drag through disordered regions. We went on to systematically test the abovementioned hypotheses.

## The concentration-dependent shift in SEC is resin and salt-dependent

First, we acquired an HSQC spectrum of $\zeta_{cyt}$ in P-6DG gel-filtration resin (BioRad) to mimic SEC conditions for NMR spectroscopy (Fig. 3c). The line widths of resonances were broad, reflecting long rotational correlation times due to spatial confinement, but the chemical shifts and relative intensities of resonances were nearly identical with the ones free in solution. We were thus able to eliminate the possibility of crowding-induced dimerization under SEC conditions.

Second, in case that the concentration-dependent shift of the elution volume we observed for $\zeta_{cyt}$ and CD3ε was caused by overloading of the gel-filtration column at high concentrations (100 μl of 400 μM protein, i.e., ~0.5 mg $\zeta_{cyt}$ under our conditions), the same shift should be observable for other proteins as well. We tested this hypothesis with Gli3-90, a 90-amino-acid fragment of the largely IDP Gli3, which is disordered in solution. Its elution volume did not shift as a function of loading concentration (Fig. 3b), suggesting that a shift is not typical for disordered proteins in general but specific for $\zeta_{cyt}$– and CD3ε.

Third, to test whether an interaction with the resin or other parts of the column leads to the observed shift, we switched from the cross-linked agarose and dextran resin of the Superdex 75 column to a Shodex KW-803 column with a silica matrix. Unexpectedly, the $M^{app}$ at low micromolar concentration of $\zeta_{cyt}$ was close to the theoretical monomer M of 13,157 Da in 20 mM potassium phosphate buffer (pH 7.0) at 150 mM NaCl (Fig. 3d). Depending on their amino acid composition, IDPs usually have larger hydrodynamic radii than folded proteins of the same M and therefore are expected to elute at higher $M^{app}$ [36]. Between 50 and 100 μM loading concentration, the $M^{app}$ plateaued at ~20,000 Da, that is, too small for a $\zeta_{cyt}$ dimer (theoretical M of 26,314 Da). These data indicated that the shift was not caused by dimerization, in agreement with NMR, AUC and MALS data.

Fourth, because we had observed the concentration-dependent shift with two types of resins, we considered the possibility of non-ideal protein behavior at higher protein concentrations. As such behavior strongly depends on solution conditions, we varied the salt concentration and investigated the concentration-dependent elution volume at low and high salt concentrations [20 mM potassium phosphate (pH 7) with 0 M or 1 M NaCl, respectively; Fig. 3d]. In low salt, the $M^{app}$ varied between 4200 and 26,000 Da, which are inconsistent with a monomer–dimer equilibrium, as the lower $M^{app}$ is well below the theoretical M of $\zeta_{cyt}$. These data demonstrate that the elution volume at low concentration is shifted, while it may be normal at high concentration. High salt was able to quench the concentration-dependent shift nearly completely. High salt also reduced the shift for CD3ε (Fig. 3e). In 1 M NaCl, the MALS profile is consistently indicative of a monomeric state (Fig. 3f). These SEC-MALS data at different salt concentrations together with AUC and NMR data clearly demonstrate that $\zeta_{cyt}$ does not dimerize with low micromolar dissociation constant but is mostly a monomer at physiologically relevant concentrations and that the behavior in SEC is not caused by dimerization but rather by non-standard behavior of the protein at low concentration.

Sigalov *et al.* reported the absence of a concentration-dependent shift in 6 M GdmCl and a monomer-like $M^{app}$. Our data suggest that the high ionic strength would have been enough to quench the shift and the denaturant not required. Also, we found that it was important to calibrate the column at different salt concentrations, or the $M^{app}$ at high salt would have been close to the theoretical monomer M. $\zeta_{cyt}$ and CD3ε are enriched in charged residues (see Supplemental Material, Table S1), and their hydrodynamic radii are thus expected to be highly salt dependent as net charge per residue is the strongest determinant of the compactness of IDPs [37–39]. An $M^{app}$ of 25 kDa as observed for $\zeta_{cyt}$ at high salt is in agreement with an extended conformation enabled via screening of electrostatic interactions.

We considered whether non-ideal attractive or repulsive interactions could explain the unusual behavior in SEC. AUC is a powerful method for revealing non-ideality and allows the extraction of second virial coefficients and non-ideality coefficients for sedimentation and diffusion. We did not see strong

indications for non-ideality in our data; all coefficients were relatively small. We thus conclude that $\zeta_{cyt}$ and CD3ε interact weakly with gel-filtration resin in a salt- and concentration-dependent manner and may also behave slightly non-ideally. Interestingly, the interaction is only obvious at low protein concentrations suggesting that few interaction sites are available on the column. Upon their saturation, the rest of the protein seems to behave similar to a normal IDP. As there seem to be only few sites, they may not be on the resin but, for example, on a minor resin by-product. This may explain why we observed a $V_{el}$ shift for two different resins. An interaction with few available sites or a weak interaction may be obscured in NMR experiments because of ensemble averaging or by the broad line width of resonances in resin, respectively, and thus not obvious from these experiments.

The biophysical model that emerged from the previous reports of a largely disordered dimer [27,30] suggested multiple transient interfaces, each sampled only part of the time and therefore limiting order in the dimer [23]. Such forces would likely not lead to specific dimerization but rather higher-order oligomers or even liquid-like protein assemblies that have been suggested to be important for controlling signaling events and spatial organization in the cell [14,40,41]. Importantly, weak inter-particle interactions do not lead to discrete dimerization or in fact any discrete oligomerization but should rather be viewed as an attractive potential leading to a large number of polymeric states under certain solution conditions and can indeed cause protein interactions that favor liquid–liquid demixing or crystallization [42]. Specific dimerization of an IDP is expected to be accompanied by a disorder-to-order transition of its interface leading to differences in NMR spectra for monomer and dimer states of IDPs. Our data demonstrate that $\zeta_{cyt}$ and CD3ε do not form highly disordered complexes but are monomers in solution up to millimolar concentrations. Although many protein complexes contain functionally important disorder, this leaves the question open whether completely disordered protein dimers or any completely disordered complexes exist in nature.

## Acknowledgments

We thank R. Kriwacki, V. Uversky, M. Marzahn and E. Martin for valuable discussions and L. Lambert for technical assistance. This work was supported by a V Foundation Scholar Grant (to T.M.), the National Cancer Institute Cancer Center Support Grant P30CA21765 (at St. Jude Children's Research Hospital) and the American Lebanese Syrian Associated Charities.

## Appendix A. Supplementary data

Supplementary data to this article can be found online at http://dx.doi.org/10.1016/j.jmb.2013.09.036.

*Received 26 June 2013;*
*Received in revised form 11 September 2013;*
*Accepted 25 September 2013*
Available online 10 October 2013

***Keywords:***
intrinsically disordered protein;
fuzzy complex;
immune receptor;
analytical ultracentrifugation;
size-exclusion chromatography

***Abbreviations used:***
SEC, size-exclusion chromatography; IDP, intrinsically disordered protein; HSQC, heteronuclear single quantum coherence; PRE, paramagnetic relaxation enhancement; SV, sedimentation velocity; AUC, analytical ultracentrifugation; M, molecular mass; SE, sedimentation equilibrium; MALS, multi-angle light scattering; EDTA, ethylenediaminetetraacetic acid.

## References

[1] Dunker AK, Obradovic Z, Romero P, Garner EC, Brown CJ. Intrinsic protein disorder in complete genomes. Genome Inform Ser Workshop Genome Inform 2000;11:161–71.
[2] Ward JJ, Sodhi JS, McGuffin LJ, Buxton BF, Jones DT. Prediction and functional analysis of native disorder in proteins from the three kingdoms of life. J Mol Biol 2004;337:635–45.
[3] Dyson HJ, Wright PE. Intrinsically unstructured proteins and their functions. Nat Rev Mol Cell Biol 2005;6:197–208.
[4] Xie H, Vucetic S, Iakoucheva LM, Oldfield CJ, Dunker AK, Uversky VN, et al. Functional anthology of intrinsic disorder. 1. Biological processes and functions of proteins with long disordered regions. J Proteome Res 2007;6:1882–98.
[5] Tompa P. The interplay between structure and function in intrinsically unstructured proteins. FEBS Lett 2005;579:3346–54.
[6] Dyson HJ, Wright PE. Coupling of folding and binding for unstructured proteins. Curr Opin Struct Biol 2002;12:54–60.
[7] Wright PE, Dyson HJ. Linking folding and binding. Curr Opin Struct Biol 2009;19:31–8.
[8] Uversky VN. Natively unfolded proteins: a point where biology waits for physics. Protein Sci 2002;11:739–56.
[9] Ganguly D, Zhang W, Chen J. Synergistic folding of two intrinsically disordered proteins: searching for conformational selection. Mol BioSyst 2012;8:198–209.
[10] Tompa P, Fuxreiter M. Fuzzy complexes: polymorphism and structural disorder in protein-protein interactions. Trends Biochem Sci 2008;33:2–8.
[11] Stollar EJ, Lin H, Davidson AR, Forman-Kay JD. Differential dynamic engagement within 24 SH3 domain: peptide complexes revealed by co-linear chemical shift perturbation analysis. PLoS One 2012;7:e51282.
[12] Baker JM, Hudson RP, Kanelis V, Choy WY, Thibodeau PH, Thomas PJ, et al. CFTR regulatory region interacts with

NBD1 predominantly via multiple transient helices. Nat Struct Mol Biol 2007;14:738–45.
[13] Mittag T, Orlicky S, Choy WY, Tang X, Lin H, Sicheri F, et al. Dynamic equilibrium engagement of a polyvalent ligand with a single-site receptor. Proc Natl Acad Sci USA 2008;105:17772–7.
[14] Li P, Banjade S, Cheng HC, Kim S, Chen B, Guo L, et al. Phase transitions in the assembly of multivalent signalling proteins. Nature 2012;483:336–40.
[15] Rauscher S, Baud S, Miao M, Keeley FW, Pomes R. Proline and glycine control protein self-organization into elastomeric or amyloid fibrils. Structure 2006;14:1667–76.
[16] Mittag T, Marsh J, Grishaev A, Orlicky S, Lin H, Sicheri F, et al. Structure/function implications in a dynamic complex of the intrinsically disordered Sic1 with the Cdc4 subunit of an SCF ubiquitin ligase. Structure 2010;18:494–506.
[17] Borg M, Mittag T, Pawson T, Tyers M, Forman-Kay JD, Chan HS. Polyelectrostatic interactions of disordered ligands suggest a physical basis for ultrasensitivity. Proc Natl Acad Sci USA 2007;104:9650–5.
[18] Nash P, Tang X, Orlicky S, Chen Q, Gertler FB, Mendenhall MD, et al. Multisite phosphorylation of a CDK inhibitor sets a threshold for the onset of DNA replication. Nature 2001;414:514–21.
[19] Tang X, Orlicky S, Mittag T, Csizmok V, Pawson T, Forman-Kay JD, et al. Composite low affinity interactions dictate recognition of the cyclin-dependent kinase inhibitor Sic1 by the SCFCdc4 ubiquitin ligase. Proc Natl Acad Sci USA 2012;109:3287–92.
[20] Engels N, Engelke M, Wienands J. Conformational plasticity and navigation of signaling proteins in antigen-activated B lymphocytes. Adv Immunol 2008;97:251–81.
[21] Mohan A, Sullivan WJ, Radivojac P, Dunker AK, Uversky VN. Intrinsic disorder in pathogenic and non-pathogenic microbes: discovering and analyzing the unfoldomes of early-branching eukaryotes. Mol BioSyst 2008;4:328–40.
[22] Sigalov AB. Protein intrinsic disorder and oligomericity in cell signaling. Mol BioSyst 2010;6:451–61.
[23] Mittag T, Kay LE, Forman-Kay JD. Protein dynamics and conformational disorder in molecular recognition. J Mol Recognit 2010;23:105–16.
[24] Uversky VN. Multitude of binding modes attainable by intrinsically disordered proteins: a portrait gallery of disorder-based complexes. Chem Soc Rev 2011;40:1623–34.
[25] Fuxreiter M. Fuzziness: linking regulation to protein dynamics. Mol BioSyst 2012;8:168–77.
[26] Herbert C, Schieborr U, Saxena K, Juraszek J, De Smet F, Alcouffe C, et al. Molecular mechanism of SSR128129E, an extracellularly acting, small-molecule, allosteric inhibitor of FGF receptor signaling. Cancer Cell 2013;23:489–501.
[27] Sigalov A, Aivazian D, Stern L. Homooligomerization of the cytoplasmic domain of the T cell receptor zeta chain and of other proteins containing the immunoreceptor tyrosine-based activation motif. Biochemistry 2004;43:2049–61.
[28] Germain RN. T-cell signaling: the importance of receptor clustering. Curr Biol 1997;7:R640–4.
[29] Molnar E, Deswal S, Schamel WW. Pre-clustered TCR complexes. FEBS Lett 2010;584:4832–7.
[30] Sigalov AB, Zhuravleva AV, Orekhov VY. Binding of intrinsically disordered proteins is not necessarily accompanied by a structural transition to a folded form. Biochimie 2007;89:419–21.
[31] Jaravine VA, Zhuravleva AV, Permi P, Ibraghimov I, Orekhov VY. Hyperdimensional NMR spectroscopy with nonlinear sampling. J Am Chem Soc 2008;130:3927–36.
[32] Clore GM, Tang C, Iwahara J. Elucidating transient macromolecular interactions using paramagnetic relaxation enhancement. Curr Opin Struct Biol 2007;17:603–16.
[33] Taylor IA, Eccleston JF, Rittinger K. Sedimentation equilibrium studies. Methods Mol Biol 2004;261:119–36.
[34] Zhao H, Brautigam CA, Ghirlando R, Schuck P. Overview of current methods in sedimentation velocity and sedimentation equilibrium analytical ultracentrifugation. Curr Protoc Protein Sci 2013;71:20.12.1–20.12.49.
[35] Brown PH, Schuck P. Macromolecular size-and-shape distributions by sedimentation velocity analytical ultracentrifugation. Biophys J 2006;90:4651–61.
[36] Uversky VN. Size-exclusion chromatography in structural analysis of intrinsically disordered proteins. Methods Mol Biol 2012;896:179–94.
[37] Mao AH, Crick SL, Vitalis A, Chicoine CL, Pappu RV. Net charge per residue modulates conformational ensembles of intrinsically disordered proteins. Proc Natl Acad Sci USA 2010;107:8183–8.
[38] Müller-Späth S, Soranno A, Hirschfeld V, Hofmann H, Ruegger S, Reymond L, et al. From the cover: charge interactions can dominate the dimensions of intrinsically disordered proteins. Proc Natl Acad Sci USA 2010;107:14609–14.
[39] Marsh JA, Forman-Kay JD. Sequence determinants of compaction in intrinsically disordered proteins. Biophys J 2010;98:2383–90.
[40] Brangwynne CP, Mitchison TJ, Hyman AA. Active liquid-like behavior of nucleoli determines their size and shape in *Xenopus laevis* oocytes. Proc Natl Acad Sci USA 2011;108:4334–9.
[41] Weber SC, Brangwynne CP. Getting RNA and protein in phase. Cell 2012;149:1188–91.
[42] Solovyova A, Schuck P, Costenaro L, Ebel C. Non-ideality by sedimentation velocity of halophilic malate dehydrogenase in complex solvents. Biophys J 2001;81:1868–80.
[43] Battiste JL, Wagner G. Utilization of site-directed spin labeling and high-resolution heteronuclear nuclear magnetic resonance for global fold determination of large proteins with limited nuclear Overhauser effect data. Biochemistry 2000;39:5355–65.
[44] Salmon L, Nodet G, Ozenne V, Yin G, Jensen MR, Zweckstetter M, et al. NMR characterization of long-range order in intrinsically disordered proteins. J Am Chem Soc 2010;132:8407–18.
[45] Cannon KS, Or E, Clemons WM, Shibata Y, Rapoport TA. Disulfide bridge formation between SecY and a translocating polypeptide localizes the translocation pore to the center of SecY. J Cell Biol 2005;169:219–25.